

MODEL PREDICTIVE CONTROL STRATEGY FOR PMSG WIND TURBINE SYSTEM USING FUZZY CONTROLLER

K.Saispandana, G.V. Marutheswar,

Professor, Department of Electrical Engineering

Sri Venkateswara University College of Engineering, Tirupathi, AndhraPradesh, India

Abstract- In recent times, the best control strategic method for control of Wind Turbine systems is Model based Predictive Control (MPC) in the view of fast dynamic responses and robustness to variation of parameters. MPC strategy is adopted to presage the future behavior and to procure optimal applied voltage to system for cost function to be minimal. It is applied for both Synchronous generator side control(SGSC) and Grid side control(GSC) of PMSG Wind Turbine system. The proposed technique is MPC using fuzzy controller. The simulation results presented in terms of Total Harmonic Distortion (THD) of current waveforms in order to show the significant improvement in performance of MPC with fuzzy controller than MPC with PI controller

Keywords: PMSG, Model Predictive Control, Fuzzy controller.

1.1. INTRODUCTION

In present trends, to meet the global energy demands the rapid expanding renewable source is Wind Energy[2]-[3]. With increasing cost of electricity from Non renewable energy sources and diversification of energy market, wind generation plays prominent role in distributed generation. Various control strategies have been implemented to enhance the reliability and efficiency of Wind generation systems as it is connected to grid. Even after disturbances wind turbine system has to be remained in connection to grid.

On the basis of the wind turbines implanted worldwide, they are generally c into two types: one is with a gearbox model, and the other is gearless model. Gearbox model consists of doubly fed induction generator (DFIG) Whereas gearless model has direct drive mechanism with permanent magnet synchronous generator. The Wind Energy Conversion System (WECS) with direct drive based permanent magnet synchronous generator (PMSG)[3] is one of the propitious wind energy generation systems. Its advantages include high reliability, good thermal characteristics, low weight, low mass per unit of power and a small generator size. A typical PMSG wind turbine system model is shown in Fig 1. The kinetic energy of wind is taken by windturbine and converts into mechanical energy. The electrical energy is obtained by converting mechanical energy through PMSG. Back to back converter with bidirectional power flow is interfaced between PMSG and grid. This back to back converter system consists of both the Synchronous generator side converter and the Grid side converter which is an AC to DC and AC to DC converter.

To control the PMSG based wind Turbine system[4] the current control techniques of the GSC and the SGSC become an important part. National standard performance[5] of grid codes can be achieved by proper control methods. Many current controlling approaches have been developed specially for power electronic converters[8]. Among them, generally we use Field oriented control (FOC), Direct Torque control (DTC) for the control of SGSC, and the Direct Power Control (DPC)[9], the DPC-SVM[10] for the control of GSC.

Now a days, Model predictive control exhibits excellent performance [9]-[10] in real time computation of controlling the both SGSC and GSC[7]. MPC model can presage the system future behavior and can be selected the optimal applied voltage for minimizing the cost function

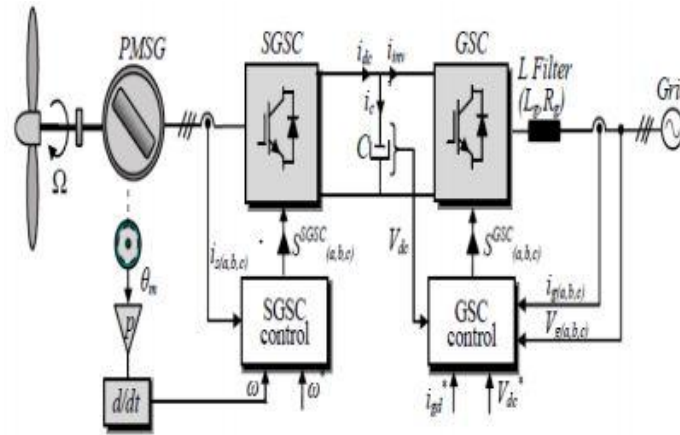


Fig.1. Wind turbine system with PMSG

1.2 PMSG MODEL

Permanent magnet in PMSG resembles the DC excitation circuit in synchronous Generator. The equivalent circuit in d and q axis is shown in Fig.2.

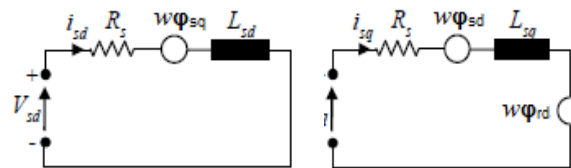


Fig.2 Equivalent circuit on d axis and q axis

The equations of the flux linkage and voltage of PMSG are given below:

$$\varphi_{sd} = L_{sd} i_{sd} + \varphi_{rd} \quad (1) \quad \varphi_{sq} = L_{sq} i_{sq} \quad (2)$$

$$V_{sd} = R_S i_{sd} + \frac{d\varphi_{sd}}{dt} - \omega_{dq} \varphi_{sq} \quad (3) \quad V_{sq} = R_S i_{sq} + \frac{d\varphi_{sq}}{dt} + \omega_{dq} \varphi_{sd} \quad (4)$$

The mechanical equations of the PMSG are expressed as follows:

$$J \frac{d\omega}{dt} = T_e - T_L - f\omega \quad (5)$$

$$T_e = \frac{3}{2} p (\varphi_{sd} i_{sq} + \varphi_{rd} i_{sq}) \quad (6)$$

Where the dq components of the stator current vector are i_{sd} and i_{sq} , the dq components of the stator flux linkage are φ_{sd} and φ_{sq} , the permanent magnet flux linkage is φ_{rd} , the dq components of the stator voltage vector are V_{sd} and V_{sq} , the angular electrical rotor speed is ω_{dq} , the rotational speed is ω , the number of pole pairs is p , the dq stator inductances are L_{sd} and L_{sq} , the stator resistance is R_S , the friction coefficient is f , inertia coefficient is J and the electromagnetic torque applied to the PMSG rotor is T_e .

1.3 .GSC MODEL

For interface between the converter and the grid, L filter is used as shown in fig 1. where L_g represents inductor and R_g represents serial resistance. The mathematical analysis of the GSC in dq axis is expressed as follows:

$$p = V_{gd} i_{gd} + V_{gq} i_{gq} \quad (7)$$

$$Q = V_{gq} i_{gd} + V_{gd} i_{gq} \quad (8)$$

$$\frac{di_{gd}}{dt} = \frac{1}{L_g} (V_{gd} - R_g i_{gd} + \omega_g L_g i_{gq} - V_{convd}) \quad (9)$$

$$\frac{di_{gq}}{dt} = \frac{1}{L_g} (V_{gq} - R_g i_{gq} - \omega_g L_g i_{gd} - V_{convq}) \quad (10)$$

Where the dq components of the current vector of grid are i_{gd} and i_{gq} , the dq components of the voltage vector of grid are V_{gd} and V_{gq} and the angular frequency of the grid voltage is ω_g . The dq components of the output voltage vector of converter are V_{convd} and V_{convq} . The inductor and resistor of the L filters are respectively L_g and R_g . The instantaneous time derivatives of grid current are di_{gd}/dt and di_{gq}/dt .

1.4 .Model Predictive Control Strategy:

MPC anticipate the change in the dependent variables of the modelled system that will be caused by the independent variables. It is based on the iterative, finite optimization of model.

MPC based algorithm controls internal current loop of both SGSC & GSC in dq synchronous reference frame. In SGSC, at minimum current, the maximum torque is obtained by setting the d component stator reference current to zero and external speed control loop uses PI controller[1]. In GSC, to impose a unity power factor, the q component grid reference current is set to zero where as d component is calculated by using PI controller in external dc link voltage control loop[1].

This project proposed the MPC based PMSG Wind turbine system with fuzzy controller in place of PI controller.

1.5 .Fuzzy Logic Controller

Fuzzy logic control system is basically composed of four major elements as shown in Fig.3. They are fuzzification interface, rule matrix, fuzzy inference engine, and defuzzification. Each block along with basic fuzzy logic operations will be explained in more detail.

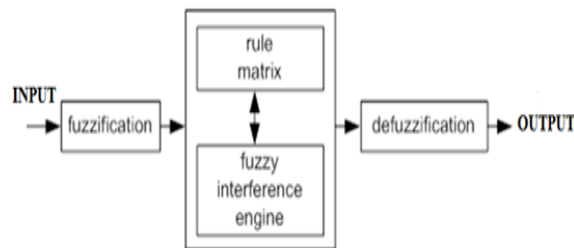


Fig.3. Block diagram for FLC

1.5.1. Fuzzification

Fuzzification involves domain transformation from crisp inputs to fuzzy inputs. Triangular membership functions with five levels are taken. As shown in Fig.4. and Fig5. the membership functions of change in error and error. These level can be described as where PS (positive small), PB (positive big), ZE (zero), NS (negative small), and NB (negative big) each level is described by fuzzy set. To obtain system best performance the membership functions has been determined by trial and error approach.

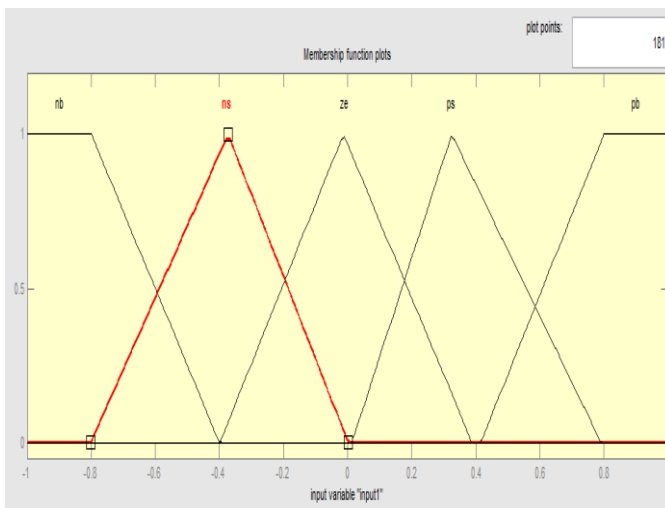


Fig.4. Membership functions of error

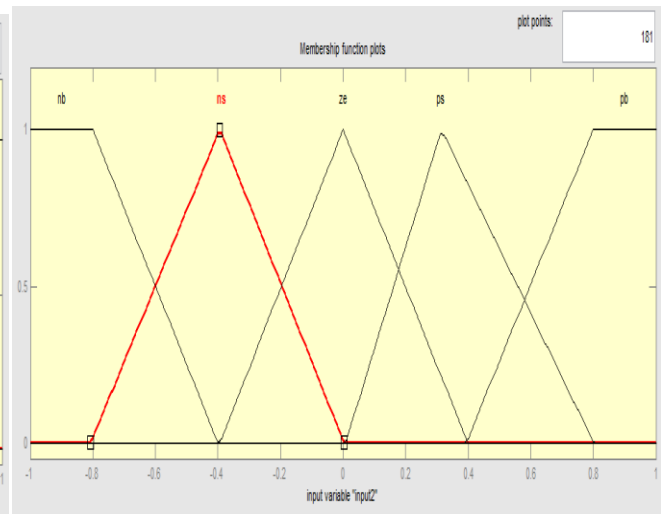


Fig.5. Membership function of change in error

The Membership functions used in fuzzy logic have different shapes or forms such as triangular, trapezoidal, generalized bell and Gaussian membership function. In many applications commonly used type of membership function is triangular. The type of the membership function can be context dependent and it is generally chosen arbitrarily according to the user experience.

1.5.2. Fuzzy Rule Base

The each input variable has five membership functions and hence a total of twenty five rules can be framed. These rules are framed in rule editor where Mamdani’s minimum implication method is employed to get the output fuzzy set for every rule.

Table.1. Control strategy based on 25 Fuzzy controls Rule with combination of five error states multiplying with five changes of error states

| Change in error | Error | | | | |
|-----------------|-------|----|----|----|----|
| | NB | NS | ZE | PS | PB |
| NB | NB | NB | NS | NS | ZE |
| NS | NB | NS | NS | ZE | PS |
| ZE | NB | NS | ZE | PS | PS |
| PS | NS | ZE | PS | PS | PB |
| PB | ZE | PS | PS | PB | PB |

1.5.3 .Fuzzy Inference

The process of creating a mapping between input and output using fuzzy logic is known as fuzzy inference shown in Fig.6.

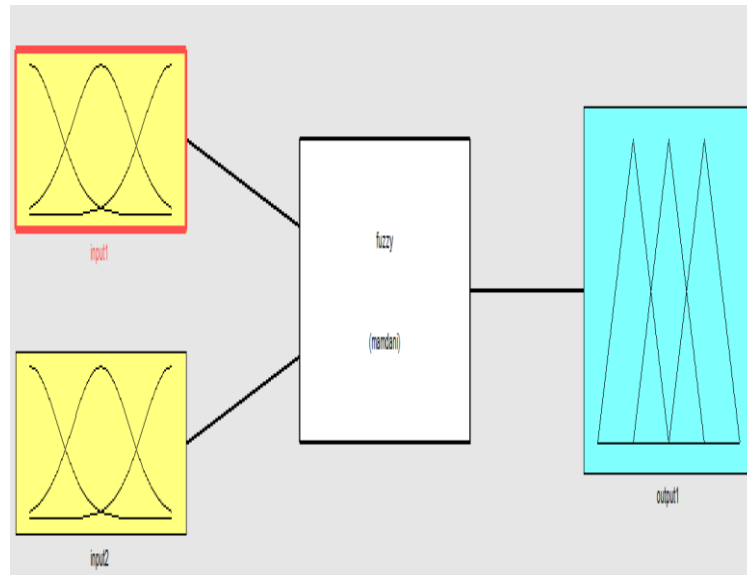


Fig.6 .Fuzzy Inference system

1.5.4 Defuzzification

The output of the inference mechanism is fuzzy output variables. The fuzzy logic controller must convert its internal fuzzy output variables into crisp values so that the actual system can use these variables. This conversion is called defuzzification. The output membership function is as in fig.7.

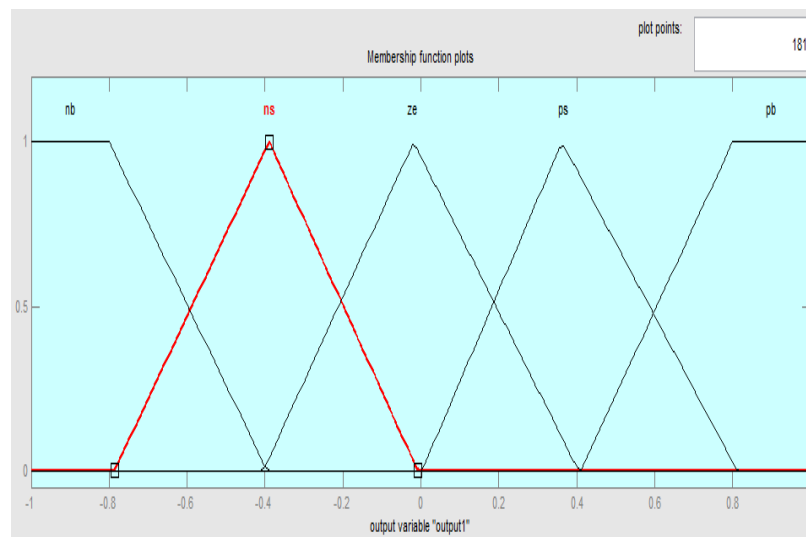


Fig.7. Output Membership function

1.6 SIMULATION RESULTS

The fixed parameters of Back to Back converter during simulation procedure were taken into account as shown in Table.2..

Table.2. Fixed parameters of Back to Back converter with PI and fuzzy controller

| Parameters | Values |
|---|-----------|
| The initially charged voltage of dc-link capacitor | 500V |
| The reference dc-link voltage V_{dc}^* was to set | 600V |
| The d axis stator current reference i_{sd}^* | Zero amps |
| The q axis current reference of grid i_{gq}^* | Zero amps |
| The speed reference of PMSG was to set | 250 rad/s |

1.5.1 Simulation results of MPC for SGSC with PI controller

The Fig.8. and Fig.9. shows the obtained simulation results of MPC for SGSC with PI controller.

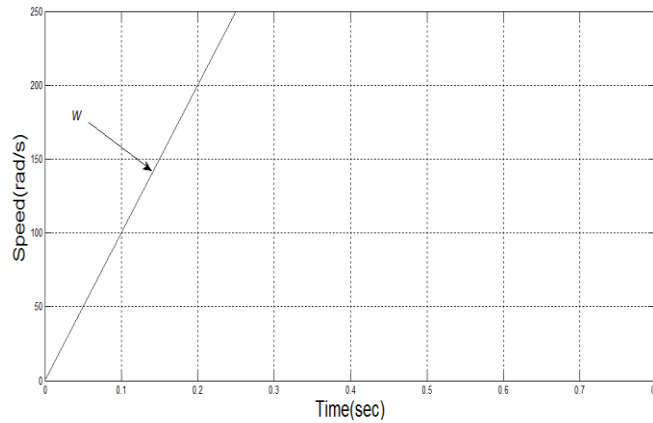


Fig.8.Simulation response of PMSG tracking performances

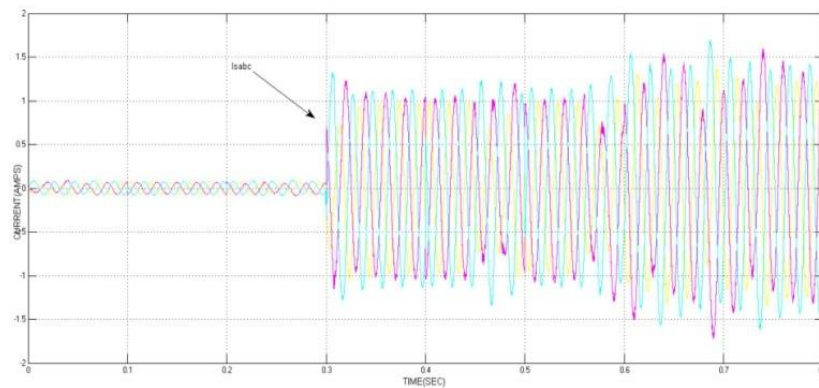


Fig.9.Simulation response of PMSG stator currents waveforms

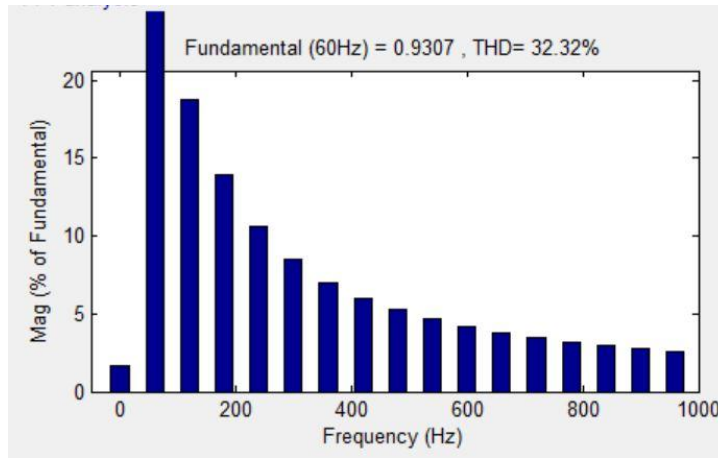


Fig.10. THD of PMSG stator current

1.5.2 Simulation results of MPC for GSC with PI controller

The Fig.11, Fig.12, Fig.13, Fig.15 and Fig.17. show the obtained Simulation results of MPC for GSC with PI controller.

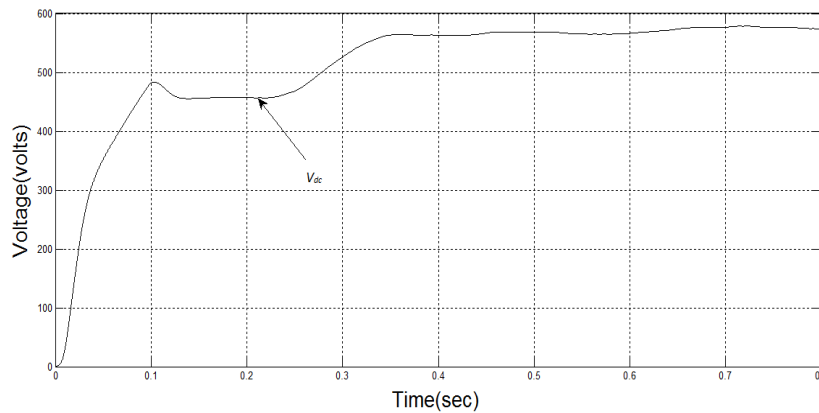


Fig.11. Simulation response of response of dc-link voltage to 600V step reference applied to the reference dc-link voltage

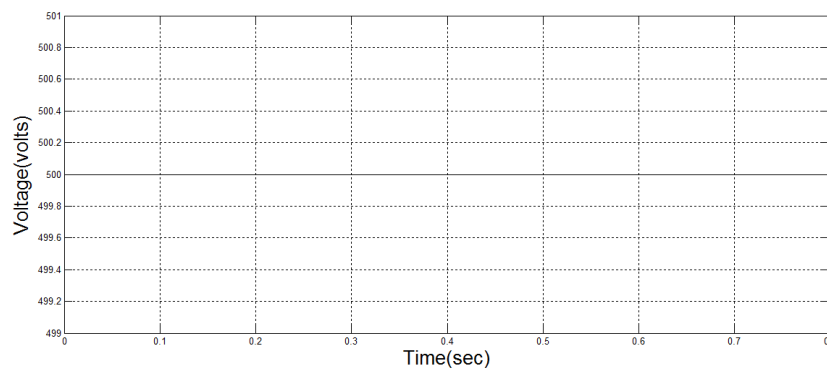


Fig.12. Simulation response of dc-link capacitor which was initially charged to 500V

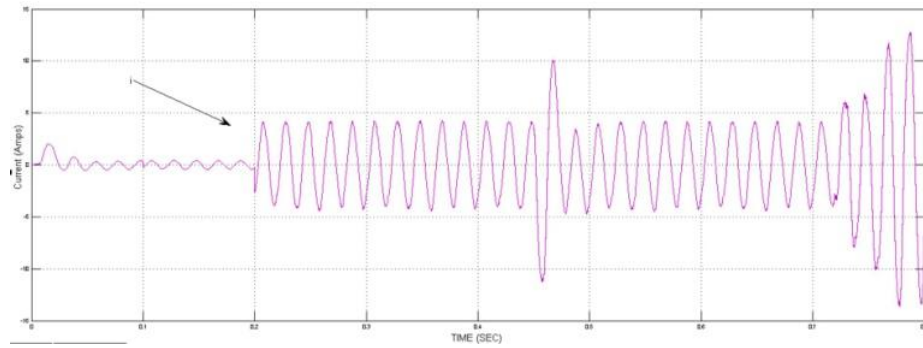


Fig.13 .Simulation response of Grid current before L_g variation

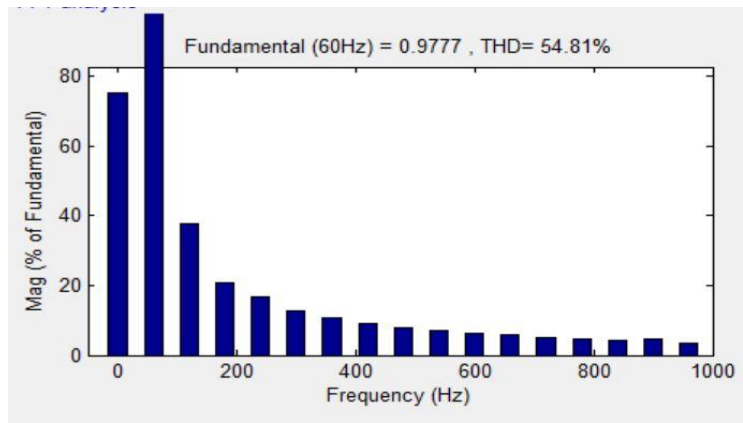


Fig.14. THD of grid current response before L_g variation

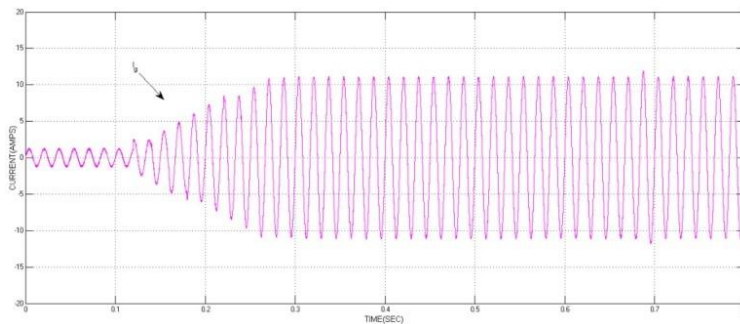


Fig.15 Simulation response of Grid current with L_g variation ($\Delta L=50\%$)

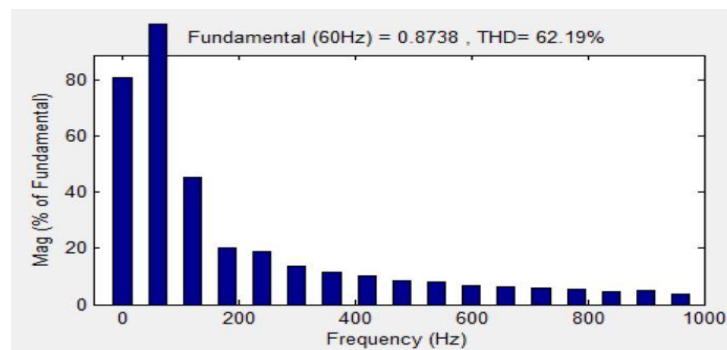


Fig.16. THD of Grid current response with L_g variation ($\Delta L=50\%$)

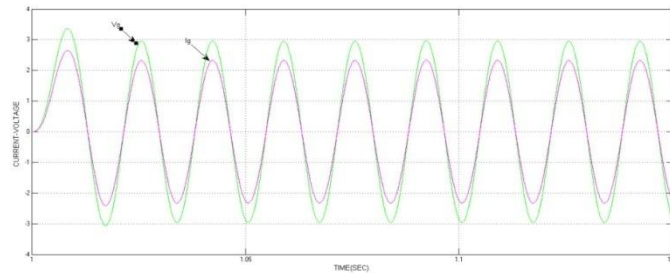


Fig.17. Simulation response of Grid voltage V_{ga} and current i_{ga} waveforms during steady state Operation

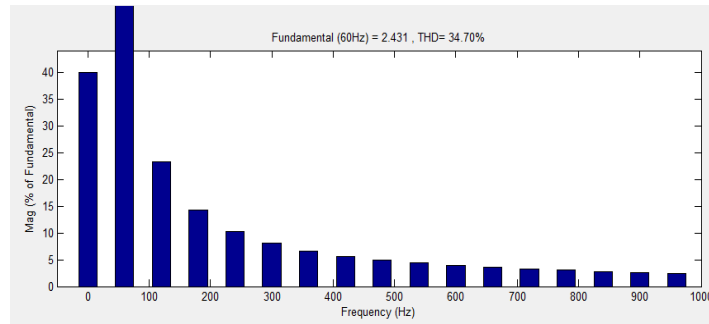


Fig.18. THD of grid current i_{ga}

1.5.3. Simulation results of MPC for SGSC with FLC

The Fig.19 and Fig.20. shows the obtained simulation results of MPC for the SGSC with FLC.

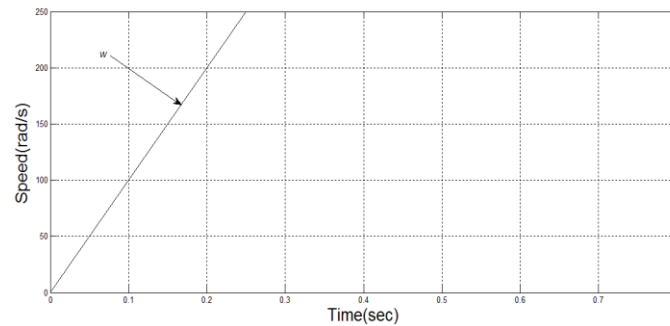


Fig.19. Simulation response of PMSG tracking performances.

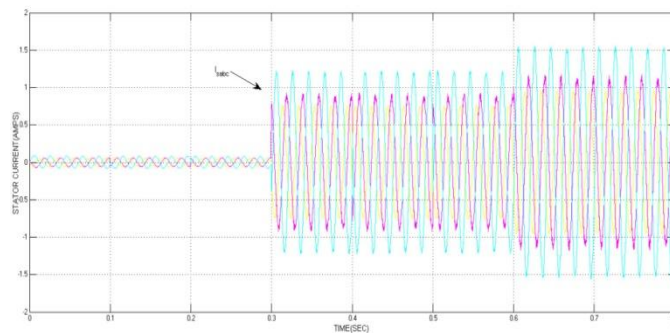


Fig.20 Simulation response of PMSG stator currents waveforms

The Fig.20. shows the PMSG stator current response. It can be noted that with increase of load torque, the stator current i_{sabc} increases

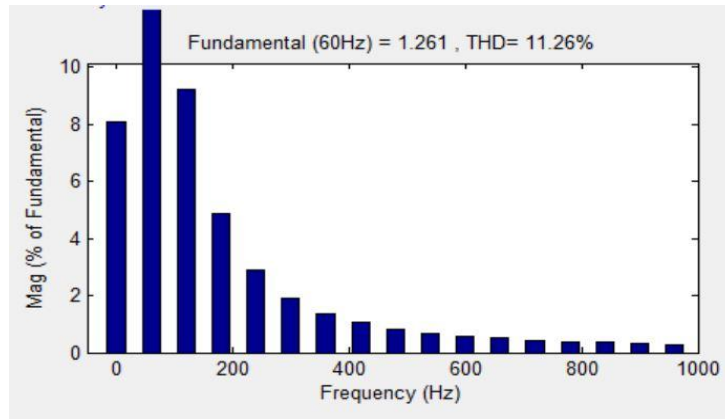


Fig.21. THD of PMSG stator current

The THD is obtained by using FFT analysis. And THD is obtained for only currents but not for the voltages. As shown in Fig.20, the obtained THD for the stator current i_{sa} was equal to 26.16%.

1.5.4. Simulation results of MPC for GSC with FLC

The Fig.21, Fig.23, Fig.24, Fig.25 and Fig.27. shows the obtained Simulation results of MPC based control for the GSC with FLC.

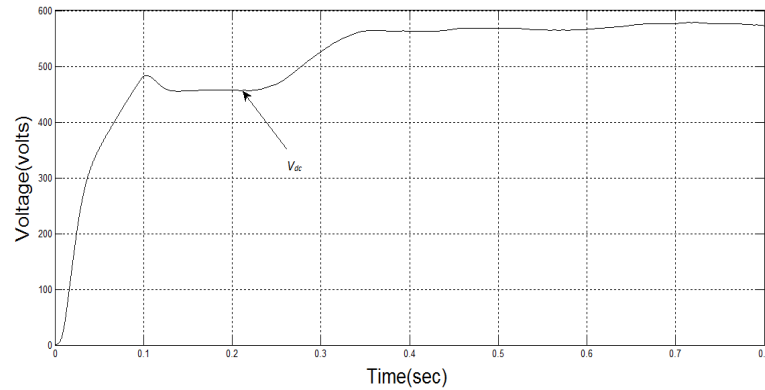


Fig.22. Simulation response of dc-link voltage response to a step reference of 600V applied to the reference dc-link voltage

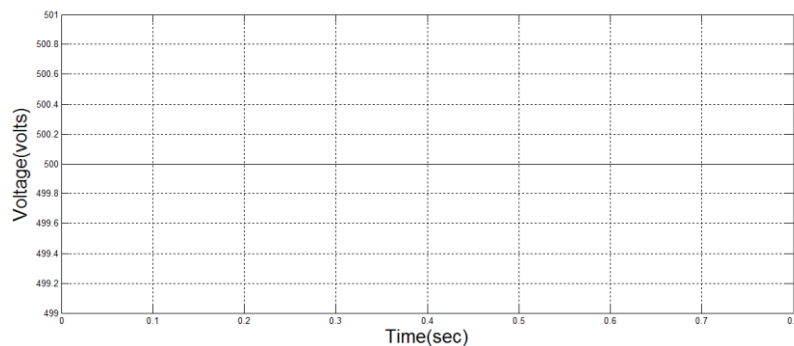


Fig.23. Simulation result of dc-link capacitor was initially charged to 500V

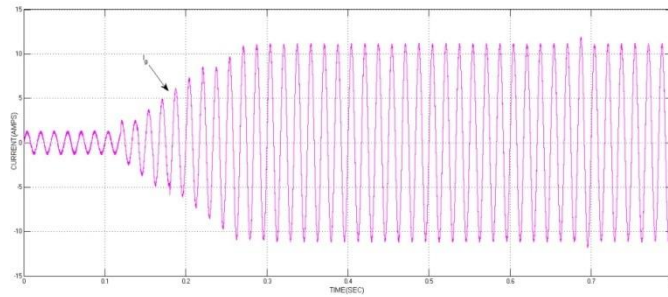


Fig.24. Simulation response of Grid current before L_g variation

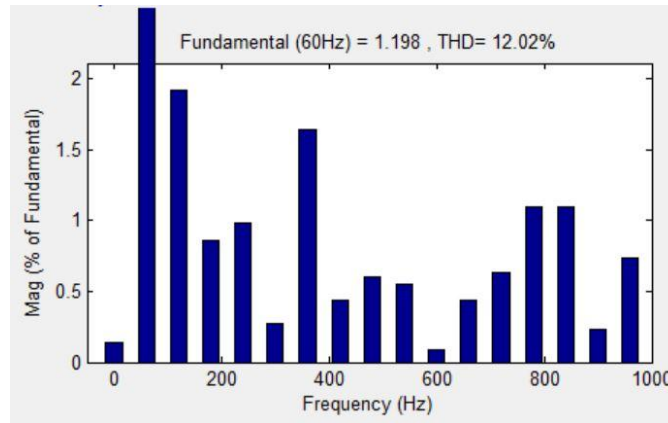


Fig.25. THD of grid current response before L_g variation

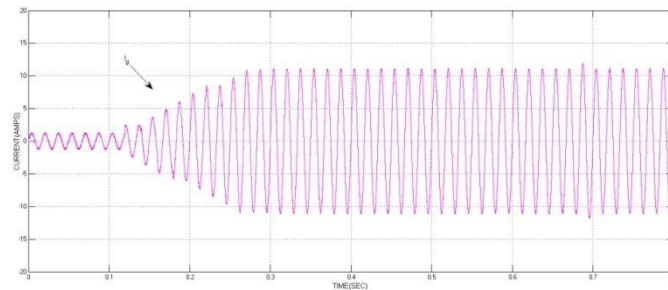


Fig.26. Simulation response of Grid current with L_g variation ($\Delta L=50\%$)

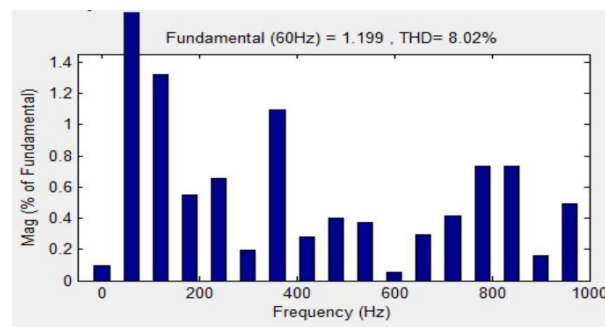


Fig.27. THD of Grid current response with L_g variation ($\Delta L=50\%$)

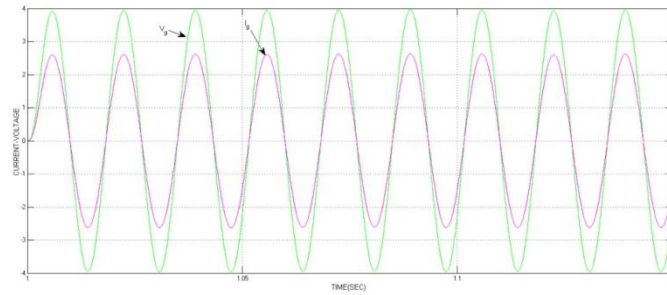


Fig.28. Simulation response of Grid voltage V_{ga} and current i_{ga} waveforms during steady state Operation

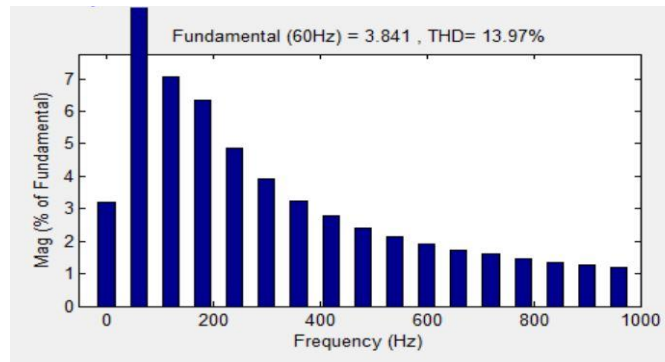


Fig.29. THD of grid current i_{ga}

Table .3. Comparison performance between PI Controller and FLC

| S.No. | Variable Name | PI Controller THD (%) | FLC THD (%) |
|-------|---|-----------------------|-------------|
| 1. | PMSG stator currents | 32.32 | 11.26 |
| 2. | The response of grid current before L_g variation | 54.81 | 12.02 |
| 3. | The response of grid current with L_g variation ($\Delta L = 50\%$) | 62.19 | 8.02 |
| 4. | Grid current i_g waveform during study state operation | 34.70 | 13.97 |

The table.3. shows that the FLC gives the best performance over the PI controller.

1.6. CONCLUSION

The first part is focused on control of the SGSC where the speed controller is performed via a PI controller and FLC includes an internal current control loop, which is based on the MPC current controller.

The second part is focused on control of the GSC where the dc-link voltage controller is based on a PI controller and FLC includes an internal current control loop, which is based on the MPC current controller. The results show that the fuzzy logic controller performances were better than PI controller. It has been shown that the developed MPC based controller is robust to variation in inductance and has high transient dynamic and low harmonic distorted grid current.

REFERENCES

- [1] Maaoui-Ben Hassine, M.W.Naouar, N.Mrabet-Bellaaj, “Model Based Predictive Control Strategies for Wind Turbine System Based on PMSG” IEEE 6th International Renewable Energy Congress, 2015.
- [2] F.Blaabjerg and K.Ma, “Future on Power Electronics for Wind Turbine Systems,” IEEE Journal of Emerging and Selected Topics in Power Electronics, Vol. 1, No. 3 pp, September 2013.
- [3] Z.Song, Ch.Xia, and T.Liu, “Predictive Current Control of Three-Phase Grid-Connected Converters with Constant Switching Frequency for Wind Energy Systems,” IEEE Trans.Ind. Electronic, vol. 60, no. 6,pp, Jun.2013.
- [4] J. He, Y. W. Li, and M. S. Munir, “A flexible harmonic control approach through voltage-controlled DG-grid interfacing converters,” IEEE Trans.Ind. Electronic, vol. 59, no. 1, pp. 444–455, Jan. 2012.
- [5] Z.Song, Ch.Xia, and T.Liu, “Predictive Current Control of Three-Phase Grid-Connected Converters with Constant Switching Frequency for Wind Energy Systems,” IEEE Trans.Ind. Electronic, vol. 60, no. 6, pp.2451-2464, Jun.2013.
- [6] M. Tsili and S. Papathanassiou, A review of grid code technical requirements for wind farms, IET Renewable Power Generation, vol. 3, pp. 308–332, Sept. 2009.
- [7] L.Tarisciotti, P.Zanchetta, A. Watson, S. Bifaretti, and Jon C. Clare, “Modulated Model Predictive Control for a Seven-Level Cascaded H-Bridge Back-to-Back Converter,” IEEE Trans. on industrial electronics, vol. 61, no. 10,pp, October 2014.
- [8] N. FREIRE, J.ESTIMA, A. CARDOSO,“A Comparative Analysis of PMSG Drives Based on Vector Control and Direct Control Techniques for Wind Turbine Applications,” PRZEGLAD ELEKTROTECHNICZNY (Electrical Review), ISSN 0033-2097, R. 88 NR 1a/2012.
- [9] D. Zhi, L. Xu, and B. W. Williams, “Improved direct power control of three-phase PWM converters “, Industrial Electronics, 2008. IECON 2008. 34th Annual Conference of IEEE, 2008, pp. 778-783.
- [10] M. Malinowski, M. Jasinski, and M. P. Kazmierkowski, “Simple direct power control of three-phase pwm rectifier using space-vector modulation (dpc-svm)”, IEEE L.G. Franquelo, J.Rodriguez, H.A. Young, A.Marquez and P.a.Zanchetta, “Model Predictive Control,” IEEE Trans. Ind. Electron., vol. 8, no. 1, pp. 16–31, Mar. 2014.